INTERNATIONAL JOURNAL FOR NUMERICAL METHODS IN ENGINEERING
Int. J. Numer. Meth. Engng 2000; **00**:1–6 *Prepared using* nmeauth.cls *[Version: 2002/09/18 v2.02]*

Coupling of a non-overlapping domain decomposition method for a nodal Finite Element Method with a Boundary Element Method

Y. Boubendir[1,*] , A. Bendali[2] & M. B. Fares[3]

[1] *School of Mathematics, University of Minnesota, 127 Vincent Hall, 206 Church St. S. E., Minneapolis, MN 55455, USA.*
[2] *INSA, Laboratoire MIP, UMR 5640, INSA-CNRS-UPS, INSA (GMM), 135 avenue de Rangueil, 31077 Toulouse Cedex 4, France & CERFACS, 42 avenue de Coriolis, 31057 Toulouse Cedex 1, France.*
[3] *CERFACS, 42 avenue de Coriolis, 31057 Toulouse Cedex 1, France.*

SUMMARY

Non-overlapping domain decomposition techniques are used both to solve the finite element equations and to couple them with a boundary element method. A suitable approach dealing with finite element nodes common to more than two subdomains, the so-called cross-points, endows the method with the following advantages. It yields a robust and efficient procedure to solve the equations resulting from the discretization process. Only small size finite element linear systems and a dense linear system related to a simple boundary integral equation are solved at each iteration and each of them can be solved in a stable way. We also show how to choose the parameter definining the augmented local matrices in order to improve the convergence. Several numerical simulations in 2D and 3D validating the treatment of the cross-points and illustrating the strategy to accelerate the iterative procedure are presented.

1. Introduction

Several methods have been devised in the last couple of years to solve the large size linear systems arising from the discretization of time harmonic scattering problems (see for example [1, 2, 3, 4, 5]). This is primarily because of the oscillatory character of the solution which accordingly requires resorting to very refined meshes. In addition, the lack of strong coercive properties of the underlaying equations, as compared for instance to those occurring in structural mechanics problems, seriously damages the efficiency of the usual solvers. This partly explains why various domain decomposition techniques have been proposed to deal with such a class of problems (e.g., [6, 3, 4, 5, 7]). The aim of this paper is to contribute to this circle of techniques. We devise a new approach for the cross-points, that is, points being shared by more that two subdomains, reducing the domain decomposition procedure to a simple and efficient iterative method for solving the nodal equations. We then show that this method adapts easily

*Correspondence to: boubendi@math.umn.edu

Received
Revised

to the coupling of a Boundary Element Method (BEM) with a Finite Element Method (FEM). In addition, we describe an algorithm called "evanescent modes damping algorithm" [9, 8], in order to suitably treat the evanescent part of the solution and thus improve the convergence of the domain decomposition method.

The techniques presented in this paper are described in the framework of the treatment of the Helmholtz equation using the non-overlapping domain decomposition method originally introduced by P.-L. Lions [15] for solutions of the Laplace equation. It was subsequently extended to time harmonic wave propagation problems by B. Després [10, 12]. In this way, we can illustrate the several advantages it owns. It reduces the large size system solution to that of several small size ones. It also allows one to construct a coupling of algorithms between different methods of discretization, such as the finite and the boundary element methods, in order to solve scattering problems involving non-homogeneous materials. The FEM deals with the finite part of the domain enclosing any heterogeneousness of the scatterer, independently from the BEM which efficiently tackles the equations describing the propagation of the wave in an infinite homogeneous medium. In contrast, the standard coupling methods yield systems of very large size having a matrix with sparse and dense blocks [14, 13] which are thus generally hard to solve. The separation of the solution in the finite part from that in the infinite one makes it possible to use special procedures to deal with the infinite region and again use non-overlapping domain decomposition in the finite part. A difficulty however appears at the level of the cross-points which are points common to several interfaces and thus to several subdomains. To overcome this difficulty, the main idea of the method we propose consists of keeping the finite elements unknowns and equations related to the cross-points. In other words, a strong coupling is maintained for the degrees of freedom carried by the cross-points for both the unknowns and the testing functions. In this way, no nodal value is introduced for the interface unknowns at these points. Such an idea has been already used in several contexts [16, 18, 19] but not as it is delt with here. This point is detailed in [20] where a theoretical study of this method is carried out. In contrast to a strict domain decomposition procedure, the local problems remain coupled at the cross-points. However, since their number is relatively small, even when compared to the size of the local problems, a Schur complement procedure deals with the coupling as a simple post-processing completing each iteration. The stability and the convergence of this algorithm are proved in [20].

The lack of coerciveness of the Helmholtz equation, already mentioned, has given rise to new developments on Després' algorithm with, as an objective, the improvement of the convergence of the related iterative procedure. Such an improvement is based on the construction of more adapted transmission conditions on the artificial interfaces [4, 5] than those initially proposed by Després. In this respect, we have introduced a modification of these conditions to construct an algorithm, named "the evanescent modes damping algorithm" [9, 36], which, while having much better convergence properties, consists of a simple modification of the parameter involved in Després' initial algorithm. Indeed, numerical simulations demonstrate the weak dependance of the iteration number with respect to the frequency or to mesh refinement. Even more, we will see that, for the 3D case, the algorithm seems to own better convergence properties that for the 2D one. This is in contrast with some direct methods based on multi-frontal Gauss eliminations (see, for example, [29, 28] for an account on such a method) where the excessive increase in memory storage in 3D may lead to a complete failure of the solving procedure.

This paper is organized as follows. The two first sections are respectively devoted to the description of a model scattering problem, the standard way to solve it by a coupling of a FEM

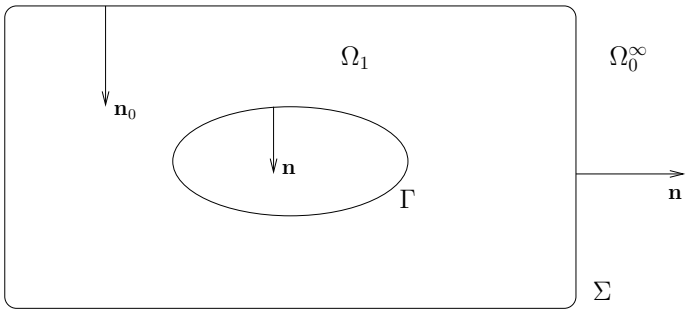

Figure 1. A typical geometry.

with a BEM, and to the description of the non-overlapping domain decomposition method used in this paper at the level of the boundary-value problem. In a third section, the approach is described at the discrete level. More particularly, it is shown how the difficulty arising from the cross-points can be overcome and how the same domain decomposition techniques can be used to efficiently couple the FEM with the BEM. The fourth section is devoted to the choice of the transmission parameter (or equivalently the choice of the way to augment the local matrices) to improve the convergence properties of the method. In a final section, the results of various numerical experiments in 2D and 3D are given to validate the overall procedure.

2. A model problem in the scattering of time harmonic waves

For the sake of simplicity, we limit ourselves to the consideration of the scattering of a two-dimensional time-harmonic wave by a possibly imperfectly conducting cylinder represented by a closed curve Γ of the plane covered by an heterogeneous dielectric occupying the domain Ω externally bounded by a closed curve Σ. However, as indicated at the end of this study, the techniques, that are used here, also apply to a 3D acoustic wave in a straightforward way. We will give below the adaptations, required to deal with this case, as well as the results related to some numerical experiments carried out in the framework of a parallelized solver code.

The wave propagates in the unbounded domain Ω_0^∞, whose boundary is Σ. We denote by $\mathbf{n}$ (resp. $\mathbf{n}_0$) the outward unit normal to the boundary of Ω (resp. Ω_0^∞) as depicted in figure 1. For the sake of clarity, the electromagnetic field is assumed to be a TE wave, that is, an H_z-field. Denoting by u and u_0 the z-components of the magnetic field related to the total wave in Ω and Ω_0^∞ respectively, we can state the scattering problem as follows

$$\left\{\begin{array}{l} \nabla\cdot(\dfrac{1}{\varepsilon}\nabla u)+k^2\dfrac{n^2}{\varepsilon}u=0 \quad \text{in } \Omega\subset\mathbb{R}^2,\\ \Delta u_0+k^2u_0=0 \quad \text{in } \Omega_0^\infty\subset\mathbb{R}^2,\\ \varepsilon^{-1}\partial_{\mathbf{n}}u=0 \quad \text{on } \Gamma,\\ \lim\limits_{|x|\to+\infty}|x|^{1/2}\left(\nabla(u_0-u^{\text{inc}})\cdot\dfrac{x}{|x|}-ik(u_0-u^{\text{inc}})\right)=0, \end{array}\right. \tag{1}$$

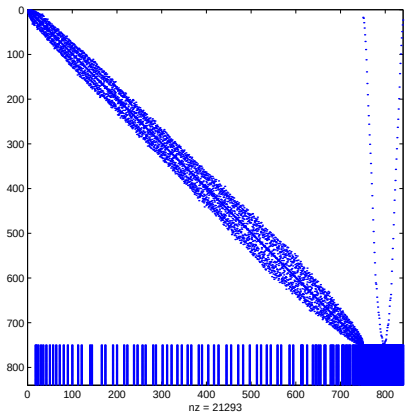

Figure 2. Structure of matrix corresponding to a direct coupling procedure

where $\Delta := \partial^2_{x_1} + \partial^2_{x_2}$ is the usual laplacian in two dimensions, k is the wave number, and n and ε are respectively the index and the relative permittivity of the dielectric medium filling Ω. Finally, system (1) is supplemented with the following transmission conditions

$$u_0 - u = 0 \quad \text{on } \Sigma, \tag{2}$$

$$\partial_{\mathbf{n}_0} u_0 + \varepsilon^{-1} \partial_{\mathbf{n}} u = 0 \quad \text{on } \Sigma. \tag{3}$$

Under the following hypotheses on n and ε, assumed to be in $L^\infty(\Omega)$,

$$\Re e(\varepsilon) \text{ and } \Re e(n) \geq 1, \quad \Im m(\varepsilon) \text{ and } \Im m(n) \geq 0,$$

the problem (1)–(3) is well posed [42, 22].

To solve this kind of scattering problem, the usual techniques consist of coupling a (FEM) to deal with the variable coefficients problem set in Ω with a (BEM) for the problem posed in Ω_0^∞ [14, 13, 8]. More precisely, the main steps of these coupling procedures can be brought out as follows. First, the auxiliary unknown

$$p := \partial_{\mathbf{n}_0} u_0|_\Sigma = -\varepsilon^{-1} \partial_{\mathbf{n}} u|_\Sigma \tag{4}$$

is considered. Next, the variable coefficients Helmholtz equation in Ω, as well as the Neumann-like boundary conditions on Γ and Σ are variationally expressed:

$$a_\Omega(u, v) + \int_\Sigma pv \, d\Sigma = 0, \tag{5}$$

with

$$a_\Omega(u, v) := \int_\Omega \varepsilon^{-1} \left(\nabla u \cdot \nabla v - k^2 n^2 uv \right) d\Omega, \tag{6}$$

and v a test function. In order to use a BEM for solving the problem in Ω_0^∞, we express u_0 by means of an appropriate integral representation

$$u_0(x) = u^{\text{inc}}(x) + Vp(x) + Nu(x) \quad x \in \Omega_0^\infty \tag{7}$$

where respectively Vp and Nu are the single- and the double-layer potential respectively associated with densities p and $u|_\Sigma$

$$Vp(x) := \int_\Sigma G(x,y)p(y)\,d\Sigma_y, \quad Nu(x) := -\int_\Sigma \partial_{\mathbf{n}_0(y)}G(x,y)u(y)\,d\Sigma_y, \tag{8}$$

and $G(x,y) := (i/4)H_0^{(1)}(k\,|x-y|)$ is the Green kernel yielding the integral representation of the outgoing solutions to the Helmholtz equation, $H_0^{(1)}$ being the first kind Hankel function of order 0. Taking in (7) the trace of u_0 on Σ, thanks to the usual jump relations (see, for example, [25, 40, 41]), we readily come to the following integral equation on Σ

$$-(\tfrac{1}{2} - N)u(x) + Vp(x) = -u^{\text{inc}}(x), \quad \text{for } x \in \Sigma. \tag{9}$$

Joining equation (5) with (9), we obtain the formulation

$$\begin{cases} a_\Omega(u,v) + \displaystyle\int_\Sigma pv\,d\Sigma = 0, \\ 2\displaystyle\int_\Sigma Vp\ q\,d\Sigma + \int_\Sigma (2N-1)uq\,d\Sigma = -2\int_\Sigma u^{\text{inc}}q\,d\Sigma, \end{cases} \tag{10}$$

where q is a test function. An appropriate FEM discretization for u and v and a BEM one for p and q classically brings back the solution of (10) to that of a linear system. This linear system is composed of three parts: a sparse matrix generated by the FEM, a dense one related to the BEM and a last part, partly sparse and partly dense, which couples the FEM with the BEM (see figure 2). For large size problems, as those concerning a relatively high frequency or those requiring a full waves three-dimensional modeling, the main difficulty comes from the high cost in computing time and memory storage which are then necessary to solve the linear system. In particular, the parallelization strategies are not well adapted to the above matrix structure [35]. In addition, without the use of a special combined integral equation, the formulation (10) can be corrupted by some spurious modes [35]. The non-overlapping domain decomposition method makes it possible to avoid all of these difficulties at once.

3. Non-overlapping continuous domain decomposition method.

We uncouple the exterior problem in Ω_0^∞ from the interior one in Ω using a non-overlapping domain decomposition method. We are specifically interested in the method, introduced by P.-L. Lions [15] in the context of the Laplace equation and adapted to wave propagation problems by B. Després [6], which consists of combining the continuity conditions (2)-(3) in the following form

$$\varepsilon^{-1}\partial_{\mathbf{n}}u + \mathcal{S}u = -\partial_{\mathbf{n}_0}u_0 + \mathcal{S}u_0 \quad \text{on } \Sigma, \tag{11}$$

$$\partial_{\mathbf{n}_0}u_0 + \mathcal{S}u_0 = -\varepsilon^{-1}\partial_{\mathbf{n}}u + \mathcal{S}u \quad \text{on } \Sigma, \tag{12}$$

where $\mathcal{S}$ is an appropriate invertible operator. The equivalent writing of the transmission conditions (11)-(12) makes it possible to solve problem (1) through the following iterative

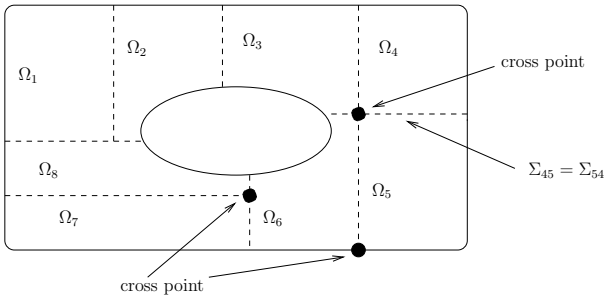

Figure 3. Partition of the initial domain.

process

$$\begin{cases} \Delta u_0^{(n+1)} + k^2 u_0^{(n+1)} = 0 \quad \text{in } \Omega_0^\infty, \\ \lim\limits_{|x|\to+\infty} |x|^{1/2} \left(\nabla(u_0^{(n+1)} - u^{\text{inc}}) \cdot \dfrac{x}{|x|} - ik(u_0^{(n+1)} - u^{\text{inc}}) \right) = 0, \end{cases} \tag{13a}$$

$$\partial_{\mathbf{n}_0} u_0^{(n+1)} + \mathcal{S} u_0^{(n+1)} = g_0^{(n)} \quad \text{on } \Sigma, \tag{13b}$$

$$\begin{cases} \nabla \cdot (\dfrac{1}{\varepsilon} \nabla u^{(n+1)}) + k^2 \dfrac{n^2}{\varepsilon} u^{(n+1)} = 0 \quad \text{in } \Omega_1, \\ \varepsilon^{-1} \partial_{\mathbf{n}} u^{(n+1)} = 0 \quad \text{on } \Gamma, \end{cases} \tag{14a}$$

$$\varepsilon^{-1} \partial_{\mathbf{n}} u^{(n+1)} + \mathcal{S} u^{(n+1)} = g^{(n)} \quad \text{on } \Sigma, \tag{14b}$$

where

$$\begin{aligned} g_0^{(n)} &= -\varepsilon^{-1} \partial_{\mathbf{n}} u^{(n)} + \mathcal{S} u^{(n)}, \quad g^{(n)} = -\partial_{\mathbf{n}_0} u_0^{(n)} + \mathcal{S} u_0^{(n)}, \\ g_0^{(n+1)} &= -\varepsilon^{-1} \partial_{\mathbf{n}} u_1^{(n+1)} + \mathcal{S} u_1^{(n+1)} = -g^{(n)} + 2\mathcal{S} u_1^{(n+1)}, \\ g^{(n+1)} &= -\partial_{\mathbf{n}_0} u_0^{(n+1)} + \mathcal{S} u_0^{(n+1)} = -g_0^{(n)} + 2\mathcal{S} u_0^{(n+1)}, \end{aligned} \tag{15}$$

can be considered as the information which has to be exchanged through the interface Σ between the domains Ω and Ω_0^∞.

The domain decomposition algorithm (13)-(14) makes it possible to deal separately with the solution in the domain Ω and the solution in the domain Ω_0^∞. This allows the use of the most adapted solution procedure for each of the boundary-value problems. For instance, the solution in Ω_0^∞ can be done through a boundary element method coupled with an efficient dense linear system solver or a fast procedure like the FMM (e.g., [1]). For nonhomogeneous dielectrics, the solution in Ω can be obtained only through a finite element method. The domain decomposition method hence appears as an efficient procedure to couple the two solution processes. This is mainly the algorithm presented in [35]. In this work, we will see that the non-overlapping domain domain decomposition method also applies for the FEM problem in Ω so that only small size FEM linear systems need to be solved at each iteration.

The first step of the non-overlapping domain decomposition method consists of splitting Ω into several subdomains Ω_i, $i = 1, \ldots, N$, such that

- $\overline{\Omega} = \bigcup_{i=1}^{N} \overline{\Omega}_i$ $(i = 1, \ldots, N)$,
- $\Omega_i \cap \Omega_j = \emptyset$, if $i \neq j$, $(i, j = 1, \ldots, N)$,
- $\partial\Omega_i \cap \partial\Omega_j = \overline{\Sigma}_{ij} = \overline{\Sigma}_{ji}$ $(i, j = 1, \ldots, N)$ is the artificial interface (figure 3) separating Ω_i from Ω_j as long as its interior Σ_{ij} is not empty.

Then, applying the Lions-Després algorithm and coupling with the exterior problem (13), the solution of the initial problem (1) is reduced to an iterative procedure, where each iteration is performed by solving the local problems

$$\left\{ \begin{array}{l} \nabla \cdot (\dfrac{1}{\varepsilon} \nabla u_i^{(n+1)}) + k^2 \dfrac{n^2}{\varepsilon} u_i^{(n+1)} = 0 \quad \text{in } \Omega_i, \\ \varepsilon_i^{-1} \partial_{\mathbf{n}_i} u_i^{(n+1)} = 0 \quad \text{on } \Gamma_i, \end{array} \right. \tag{16a}$$

$$\varepsilon_i^{-1} \partial_{\mathbf{n}_i} u_i^{(n+1)} + \mathcal{S} u_i^{(n+1)} = g_{ij}^{(n)} \quad \text{on } \Sigma_{ij}, \tag{16b}$$

the following problem posed in an unbounded domain

$$\left\{ \begin{array}{l} \Delta u_0^{(n+1)} + k^2 u_0^{(n+1)} = 0 \quad \text{in } \Omega_0^{\infty}, \\ \lim\limits_{|x| \to +\infty} |x|^{1/2} \left(\nabla (u_0^{(n+1)} - u^{\text{inc}}) \cdot \dfrac{x}{|x|} - ik (u_0^{(n+1)} - u^{\text{inc}}) \right) = 0, \end{array} \right. \tag{17a}$$

$$\partial_{\mathbf{n}_0} u_0^{(n+1)} + \mathcal{S} u_0^{(n+1)} = g_0^{(n)} \quad \text{on } \Sigma, \tag{17b}$$

and form the quantities to be transmitted through the interfaces

$$g_{ij}^{(n+1)} = -\varepsilon_j^{-1} \partial_{\mathbf{n}_j} u_j^{(n+1)} + \mathcal{S} u_j^{(n+1)} = -g_{ij}^{(n)} + 2\mathcal{S} u_j^{(n+1)} \quad \text{on } \Sigma_{ij}, \tag{18}$$

where $u_i = u|_{\Omega_i}$, $\mathbf{n}_i$ (resp. $\mathbf{n}_j$) the outward unit normal of the boundary of Ω_i (resp. Ω_j), $i = 1, \ldots, N$, $j = 0, \ldots, N$, $\varepsilon_0 = 1$, $\Gamma_i = \partial\Omega_i \cap \Gamma$, $\Sigma_{i0} = \Sigma \cap \partial\Omega_i$ and $g_0^{(n+1)}$ being defined in some special way from the $g_{i0}^{(n+1)}$. Note that the boundary condition on Γ_i does not take place if the interior of $\partial\Omega_i \cap \Gamma$ is the empty set. It is also worth mentioning that a same symbol $\mathcal{S}$ is used to denote operators acting on functions defined on different sets. These operators are actually parameters characterizing the domain decomposition method and play a crucial role in its convergence properties. By fixing the form of $\mathcal{S}$, we can hence easily describe the actual domain decomposition method that is considered.

A general partition of the domain Ω generates cross-points, that are points belonging to more that two subdomains (see figure 3). The use of nodal finite element method then requires an adequate treatment for these points. Such an issue has been addressed at the theoretical level in [20]. The next section is devoted to the description of the adaptation of this method as it is proposed here. Mainly, we explain below our approach for dealing with cross-points that are located on the interface Σ and hence are supporting nodal values related to the BEM (13).

4. Non-overlapping nodal domain decomposition method.

4.1. Nodal finite element method.

Difficulties appear with the treatment of the degrees of freedom carried by the cross-points during the iterative process [4, 8]. Two of the authors [20] have theoretically studied the

approach, which consists of preserving the finite element equation at the level of these points, i.e., maintaining a strong continuity requirement at the nodes shared by at least three subdomains. This way to proceed results in an iterative solving algorithm, which, although different, presents a slight difference only with a classical domain decomposition method. The main advantage of this algorithm is that its stability and convergence can be established theoretically (see [20] for the details). We now give the various steps of this method.

Let $\mathcal{T}^h$ and X^h be respectively a nondegenerate triangular mesh of Ω and its associated $\mathbb{P}_1$-continuous finite element space. The discrete version of problem (14a–14b) is defined as follows

$$\left\{ \begin{array}{l} u^h \in X^h,\ \forall v^h \in X^h, \\ a(u^h, v^h) = Lv^h, \end{array} \right. \tag{19}$$

where

$$a(u^h, v^h) := \int_\Omega \frac{1}{\varepsilon}(\nabla u^h \cdot \nabla v^h - k^2 n^2 u^h v^h)\, d\Omega + \int_\Sigma \mathcal{S} u^h v^h \, d\Sigma,$$
$$Lv^h := \int_\Sigma g v^h \, d\Sigma.$$

Let us now assume that $\mathcal{T}^h$ is compatible with the domain decomposition in the sense that it induces a mesh $\mathcal{T}_i^h$ on each subdomain, and introduce X_i^h as the $\mathbb{P}_1$-continuous functions approximation space of $H^1(\Omega_i)$. Any function $v_i^h \in X_i^h$ can be decomposed as follows

$$v_i^h = v_{iI}^h + \sum_{j \in \Lambda_i} v_{ij}^h + v_c^h,$$

with

- all the nodal values of v_{iI}^h are zero on the closure $\overline{\Sigma}_{ij}$ $(j \in \Lambda_i)$ of any artificial interface separating Ω_i from another subdomain Ω_j (Λ_i denotes the set of numbers j of subdomains Ω_j sharing a common interface with Ω_i),
- all the nodal values of v_{ij}^h are zero unless those located at the interior of the the artificial interface Σ_{ij} (hence excluding cross-points),
- all the nodal values of v_c^h are zero except for the nodes corresponding to a cross-point, defined here as a point on the closure of an artificial interface $\overline{\Sigma}_{ij}$ but not lying in its interior Σ_{ij}. (In this way, points which are at the junction of $\overline{\Sigma}_{ij}$ and the interface Σ separating Ω from Ω_0 or the boundary Γ of Ω are also counted as cross-points. In this respect, points located at the junction of the artificial interfaces and Γ are unduly counted as cross-points. We have however observed that this way to proceed, which, at a first sight, may appear as a convenient manner to make simpler the description and the implementation of the algorithm, improves the convergence properties of the method.)

In some way, v_{iI}^h and v_c^h can be, and are, identified to a function in X^h while the functions v_{ij}^h make it possible to relax the continuity requirement at the interfaces. We will denote by X_c^h the subspace of X^h spanned by the v_c^h.

To introduce the domain decomposition method, we consider the "broken" space X_{B}^h spanned by the functions v^h that can be written in an unique manner as

$$v^h = \sum_{i=1}^{N} \left(v_{iI}^h + \sum_{j \in \Lambda_i} v_{ij}^h \right) + v_c^h.$$

The finite element space X^h appears as the subspace of $X^h_{\rm B}$ consisting of those of the functions $v^h \in X^h_{\rm B}$ that are continuous at the nodal points on Σ_{ij}. This continuity is expressed by a matching condition which is at the heart of the domain decomposition method. Let us notice also that the forms a_Ω and L can be written as follows

$$a_\Omega(u^h, v^h) = \sum_{i=1}^N a_i(u_i^h, v_i^h), \qquad Lv^h = \sum_{i=1}^N L_i v_i^h,$$

where

$$\begin{aligned}
&u_i^h := u^h|_{\Omega_i},\\
&a_i(u_i^h, v_i^h) := \int_{\Omega_i} \frac{1}{\varepsilon_i}(\nabla u_i^h \cdot \nabla v_i^h - k^2 n_i^2 u_i^h v_i^h)\, d\Omega_i + \int_{\Sigma_{ij}} \mathcal{S} u_i^h v_i^h \, d\Sigma_{ij},\\
&L_i v_i^h := \int_{\Sigma_{ij}} g_{ij} v_i^h \, d\Sigma_{ij}, \quad \Sigma_{ij} = \Sigma \cap \partial\Omega_i.
\end{aligned}$$

Then, we show [20] that the problem (19) is equivalent to the system

$$\begin{array}{l}
a_i\left(u_{iI}^h + \sum_{j\in\Lambda_i} u_{ij}^h + u_c^h, v_{iI}^h\right) = L_i v_{iI}^h, \quad \forall v_{iI}^h \in X_i^h, \quad i = 1, \ldots, N,\\
\left\{\begin{array}{l}
a_i\left(u_{iI}^h + \sum_{\ell\in\Lambda_i} u_{i\ell}^h + u_c^h, v_{ij}^h\right)\\
\qquad + a_j\left(u_{jI}^h + \sum_{\ell\in\Lambda_j} u_{j\ell}^h + u_c^h, v_{ji}^h\right) = L_i v_{ij}^h + L_j v_{ji}^h\\
c_{ij}^h\left(S u_{ij}^h, v_{ij}^h\right) = c_{ji}^h\left(S u_{ji}^h, v_{ji}^h\right)\\
\qquad \text{for all } v_{ij}^h \in X_i^h \text{ and } v_{ji}^h \in X_j^h,\ v_{ij}^h = v_{ji}^h \text{ on } \Sigma_{ij},\ \forall\, \Sigma_{ij},
\end{array}\right.\\
\sum_{i=1}^N a_i\left(u_{iI}^h + \sum_{\ell\in\Lambda_i} u_{i\ell}^h + u_c^h, v_c^h\right) = \sum_{i=1}^N L_i v_c^h, \qquad \forall v_c^h \in X_c^h,
\end{array}$$

where $c_{ij}^h = c_{ji}^h$ is a suitable bilinear form expressing the matching condition on the traces of u_{ij}^h and u_{ji}^h on Σ_{ij} variationally. It is simply taken as the usual L^2 scalar product on Σ_{ij} in the numerical experiments which are carried out below. The matching conditions on the normal derivatives are variationally expressed by means of those on the test functions v_{ij}^h. Finally, we relax the conditions on the artificial interfaces starting from the domain decomposition method of Lions-Després [15, 6], and obtain the final system

$$\left\{\begin{array}{l}
\left.\begin{array}{l}
a_i\left(u_{iI}^h + \sum_{\ell\in\Lambda_i} u_{i\ell}^h + u_c^h, v_{iI}^h\right) = L_i v_{iI}^h, \quad \forall v_{iI}^h \in X_i^h,\\
a_i\left(u_{iI}^h + \sum_{\ell\in\Lambda_i} u_{i\ell}^h + u_c^h, v_{ij}^h\right) + c_{ij}^h\left(\mathcal{S} u_{ij}^h, v_{ij}^h\right) =\\
\qquad L_i v_{ij}^h + c_{ij}^h\left(g_{ij}, v_{ij}^h\right), \ \forall v_{ij}^h \in X_i^h,\ j \in \Lambda_i,
\end{array}\right\} \quad i = 1, \ldots, N,\\
\sum_{i=1}^N a_i\left(u_{iI}^h + \sum_{\ell\in\Lambda_i} u_{i\ell}^h + u_c^h, v_c^h\right) = \sum_{i=1}^N L_i v_c^h \quad \forall v_c^h \in X_c^h,\\
g_{ij} = -g_{ji} + 2 S u_{ji}^h|_{\Sigma_{ij}}.
\end{array}\right. \tag{20}$$

At each iteration, g_{ij} can be assumed as the boundary data on the artificial interfaces and are transmitted from one to another subdomain.

The variational system (20) can be written in matrix form

$$\begin{bmatrix} A_{11} & & & & A_{1c} \\ & A_{22} & & & A_{2c} \\ & & \ddots & & \vdots \\ & & & A_{NN} & A_{Nc} \\ A_{c1} & A_{c2} & \dots & A_{cN} & A_{cc} \end{bmatrix} \begin{bmatrix} u_1 \\ u_2 \\ \vdots \\ u_N \\ u_c \end{bmatrix} = \begin{bmatrix} g_1 \\ g_2 \\ \vdots \\ g_N \\ g_c \end{bmatrix}, \tag{21}$$

where A_{ii}, A_{ic}, A_{ci}, $i = 1, \dots, N$, are matrices related to the discretization on Ω_i and g_i the right hand side of each problem. The index "c" represents the small size coupling at the level of the cross-points. As shown below, a Schur complement procedure makes it possible to deal with the coupling as a simple postprocessing completing each iteration.

The underlying principle governing the solution of system (21) is to express each of the u_i as

$$u_i = (A_{ii})^{-1} (g_i - A_{ic} u_c) . \tag{22}$$

This permits the derivation of the following system

$$\left(A_{cc} - \sum_{i=1}^{N} A_{ci} (A_{ii})^{-1} A_{ic} \right) u_c = g_c - \sum_{i=1}^{N} A_{ci} (A_{ii})^{-1} g_i . \tag{23}$$

System (23) is small since it involves only cross-points. For effective computations, we proceed as follows

- **Initialization step**
  - perform a LU factorization on each matrix A_{ii} $(i = 1, \dots, N)$,
  - do a forward backward sweep to compute $(A_{ii})^{-1} A_{ic}$ $(i = 1, \dots, N)$,
  - form and carry out a LU factorization of $\left(A_{cc} - \sum_{i=1}^{N} A_{ci} (A_{ii})^{-1} A_{ic} \right)$.
- **For each iteration**
  - do a forward backward sweep to compute $(A_{ii})^{-1} g_i$ $(i = 1, \dots, N)$
  - form the right-hand side $g_c - \sum_{i=1}^{N} A_{ci} (A_{ii})^{-1} g_i$ and do a forward backward sweep to compute u_c
  - obtain u_i $(i = 1, \dots, N)$ from (22) by means of basic linear algebra computations.

Besides the initialization step which requires the LU factorization of small size sparse matrices only followed by some forward backward sweeps which can be regarded as some iteration steps, the main computation cost concerns the solution of two sparse linear systems $(A_{ii})^{-1} g_i$, $u_i = (A_{ii})^{-1} (g_i - A_{ic} u_c)$ and a dense one (Eq. (23)) at each iteration. If one discard the solution of the dense system related to cross-points, it is almost the same procedure in comparison with a pure domain decomposition method unless two sparse local problems are solved instead of one at each iteration. This of course results in an overcost relatively to a standard DDM but with the two additional advantages. The cross-points are safely taken into account, and, as noticed by an anonymous referee, such a treatment for these points can be seen as a coarse problem improving the convergence of the overall iterative process.

Figure 4. Cross point treatment by the coupling method

The cross-points are related to the nodes located on the boundaries $\partial\Sigma_{ij}$ of Σ_{ij}. Therefore, linear system (23) corresponds to a 0D-problem in 2D and to a 1D-problem in 3D. As a result, the CPU time for solving this system is negligible in 2D. Below, when considering some numerical experiments for the 3D case, we explain how it is dealt with in the framework of a parallel implementation of the solving procedure and give the overcost per iteration resulting from the treatment of the cross-points relatively to a standard DDM.

If one replace the exterior problem in Ω_0^∞ by an absorbing boundary condition given by a local operator as for instance a Bayliss-Turkel radiation condition (see, for instance, [33, 30]), the solution procedure with the treatment of the cross-points is exactly the method we just described with a suitable adaptation for the bilinear form a_Ω. In the context of the coupling algorithm with a BEM, as it is proposed in this paper, the approach related to the cross-points is restricted to the FEM used to solve the problem set in Ω. More precisely, the general strategy consists in partly relaxing the strong continuity requirement at a cross-point located on Σ by maintaining it at the level of the FEM only and expressing it by means of an interface unknown to satisfy the matching conditions linking the FEM and the BEM (see figure 4). Thus, only two uncoupled systems, a finite element one in the form (21) and a second one relative to a pure BEM, have to be solved at each iteration. These systems exchange only one value at each node at the end of each iteration.

The above technique can also be used in the case where the problem in Ω_0^∞ is dealt with an absorbing boundary condition expressed in terms of a non local operator on Σ (see for instance [27, 31]). Also, the solution of the BEM can be performed using an adapted non-overlapping domain decomposition method (see [32]) so that each iteration is carried out by mainly doing one iteration for the FEM and another one for the BEM. In this way, only small size systems have to be solved at each iteration.

4.2. The boundary integral equation.

The equation (18) shows that performing an iteration is reduced to computing the solution for each problem on the artificial interfaces only. The boundary element method is particularly adapted to evaluating this quantity without having to solve the boundary-value problem (17) in all of Ω_0^∞. Here, we adopt the approach developed in [23, 34] for solving boundary-value problems related to an impedance boundary. Consider the problem

$$\left\{\begin{array}{l} \Delta u_0 + k^2 u_0 = 0, \quad \text{in } \Omega_0^\infty, \\ \partial_{\mathbf{n}} u_0 + \mathcal{S} u_0 = g_0, \quad \text{on } \Sigma, \\ \lim\limits_{|x|\to+\infty} |x|^{1/2} \left(\nabla(u_0 - u^{\text{inc}}) \cdot \dfrac{x}{|x|} - ik(u_0 - u^{\text{inc}}) \right) = 0, \end{array}\right. \tag{24}$$

where, to shorten the notation, we have set $\mathbf{n} := \mathbf{n}_0$.

The integral representation of u_0 is written in the following form

$$u_0(x) = u^{\rm inc}(x) + \int_\Sigma G_0(x,y)p(x)\,d\Sigma(y) - \int_\Sigma \partial_{\mathbf{n}_y} G_0(x,y)\lambda(x)\,d\Sigma(y) \quad x \in \Omega_0^\infty,$$

in terms of a single- and a double-layer potential respectively created by the unknown densities p and λ relatively to the kernel

$$G_0(x,y) := \frac{i}{4} H_0^{(1)}(k|x-y|), \quad H_0^{(1)} := J_0 + iY_0,$$

expressed by means of Bessel J_0 and Neumann fonctions Y_0 of order 0. After solving the following variational problem involving a supplemental unknown ℓ

$$\left\{ \begin{array}{l} a(\{\lambda,p\},\{\lambda',p'\}) + b(\ell,\{\lambda',p'\}) = \int_\Sigma f\lambda' d\Sigma, \quad \forall\{\lambda',p'\}, \\ b(\ell',\{\lambda,p\}) = 0, \quad \forall \ell', \end{array} \right. \tag{25}$$

one obtains

$$u_0|_\Sigma = \ell + \lambda/2, \tag{26}$$

where the bilinear and linear forms are defined by

$$\begin{gathered} Vp(x) := \int_\Sigma G_0(x,y)p(y)\,d\Sigma(y), \quad N\lambda(x) := -\int_\Sigma \partial_{\mathbf{n}_y} G_0(x,y)\lambda(y)\,d\Sigma(y), \\ D\lambda(x) := -\partial_s V(\partial_s\lambda)(x) - k^2 V(\lambda\,\boldsymbol{\tau})(x)\cdot\boldsymbol{\tau}_x, \\ a(\{\lambda,p\},\{\lambda',p'\}) := \int_\Sigma \{D\lambda\lambda' - N\lambda p' - Np\lambda' - Vpp'\}\,d\Sigma, \\ b(\ell,\{\lambda',p'\}) := \int_\Sigma \ell\,(p' + \mathcal{S}\lambda')\,d\Sigma, \\ f := g_0 - (\partial_{\mathbf{n}} u^{\rm inc} + \mathcal{S}u^{\rm inc}), \end{gathered}$$

where $\boldsymbol{\tau}$ represents the unit tangent to Σ obtained by rotating $\mathbf{n}$ by $\pi/2$ counterclockwise and s the curvilinear abscissa in the same orientation. The operator $\mathcal{S}$ is assumed to be symmetric relatively to the scalar product of $L^2(\Sigma)$.

Meshing Σ in a polygonal curve, still denoted by Σ, with vertices on the exact curve and approximating every unknown and test function by a continuous function linear on each segment, we are lead to solve the following linear system

$$\left[\begin{array}{ccc} D & -N^{\rm T} & \mathcal{S}M \\ -N & -V & M \\ \mathcal{S}M & M & 0 \end{array} \right] \left[\begin{array}{c} \lambda \\ p \\ \ell \end{array} \right] = \left[\begin{array}{c} Mf \\ 0 \\ 0 \end{array} \right] \tag{27}$$

Now λ, p, ℓ and f are the collum-wise vectors formed by the nodal values of the respective functions at the vertices, D, N, V, Z and M are the matrices representing the bilinear forms respectively associated by the scalar product of $L^2(\Sigma)$ to operators D, N, V, $\mathcal{S}$ and the identity relatively to the nodal values. For example, masse matrix M is defined through the following relation

$$\int_\Sigma \ell p' d\Sigma = \left[\begin{array}{ccc} p'_1 & \cdots & p'_N \end{array} \right] M \left[\begin{array}{c} \ell_1 \\ \vdots \\ \ell_N \end{array} \right]$$

where $\ell_1,\ldots,\ell_N$ and and $p'_1,\ldots,p'_N$ are the respective nodal values of ℓ and p'.

The technique used computes the matrix M according to a lumping process in order to obtain a diagonal mass matrix. The unknowns p and ℓ can be directly eliminated out of the previous system (27) resulting in a single equation for λ

$$\lambda = \left(D + (\mathcal{S}N)^T + \mathcal{S}N - \mathcal{S}^2 S\right)^{-1} Mf. \tag{28}$$

The solution consists then of computing

$$\ell = M^{-1}(N - \mathcal{S}V)\lambda \tag{29}$$

to obtain $u_0|_\Sigma$ from (26).

5. Convergence of the DDM

It is well-established that the convergence properties of the DDM highly depend on an adequate choice for the operator $\mathcal{S}$ [4, 5, 8] . In Després's original algorithm [6], S is the simple scalar operator

$$\mathcal{S} := -ik. \tag{30}$$

Although, the convergence of the iterative procedure can be theoretically established, the effective convergence of the algorithm is very slow and difficult to reach in certain exemples. Indeed, most of the eigenvalues of the iteration operator are located around 1 [8]. Roughly speaking, this part of the spectrum represents the evanescent modes and, even they do not prevent the convergence of the algorithm, these modes are responsible for its slowing down at a level that it becomes completely ineffective. To overcome this drawback, Després has proposed to use a relaxation technique which slightly improves the convergence. Collino, Ghanemi and Joly [4] have carefully studied the reason why the algorithm slows down through variational techniques. They showed that using the following operator

$$\mathcal{S} := -ik\Lambda, \tag{31}$$

where Λ is non local and invertible, yields a fixed point problem related to a contraction mapping. However, the construction and the evaluation of operator Λ is costly and, more disappointing, the convergence at the discrete level is not significantly improved in comparison with the relaxed Després algorithm [8]. In fact, as shown in [5, 36, 8], the convergence is effectively improved when the evanescent part is well treated. In [37], we proposed to write $\mathcal{S}$ in the form

$$\mathcal{S} := -ik(1 + i\mathcal{X}), \tag{32}$$

where $\mathcal{X} > 0$. This algorithm is called "Evanescent modes damping algorithm" (briefly EMDA) and was analyzed in [36, 8] in the particular case of the circular geometry and for a partition of the initial domain into two subdomains respectively bounded (interior) and unbounded (exterior). From these studies, we have observed the incompatibility between the evanescent part and propagating one when introducing the parameter $\mathcal{X}$ (or, more generally, when $\mathcal{X}$ is a self-adjoint positive operator). The evanescent modes (infinitely many) are damped but the propagating ones (finite number) are amplified. For the components of the iteration operator related to the exterior subdomain, this amplification is slight and we were able to prove that all

the coefficients describing this component are less than 1 in modulus for all $\mathcal{X} > 0$. However, for the components coming from the interior subdomain, the amplification is significant in the meaning that some coefficients can be greater than 1 in modulus. This is the reason why the proof was established for $0 < \mathcal{X} \leq \mathcal{X}_{\max}$ (for details, see [36, 8]). For the effective convergence, we observed that the optimal results are obtained where $\mathcal{X} = 1/2$. Another technique which improves the convergence is based on the optimization of the rate of convergence [5, 17]. This optimization is performed for the canonical case where the domain is all of the plane and is decomposed in two half-planes. The idea consists of writing the operator $\mathcal{S}$ as

$$\mathcal{S} := \delta + \gamma \partial_s^2, \tag{33}$$

where $(\delta, \gamma) \in \mathbb{C} \times \mathbb{C}$ and ∂_s the tangential derivative operator. The geometry then permits the use of Fourier techniques to compute the rate of convergence explicitly. The results are then empirically transposed to arbitrary geometries to determine values of δ and γ, aimed to be optimal, for damping both the propagating and the evanescent modes. The principle of this approach is interesting since a rigorous determination of an operator yielding an optimal rate of convergence seems to be out of reach in this context. However several issues seem to be not satisfactorily handled. It is not clear how the parameters derived in the case of the half plane remains optimal for the other geometries in particular for non-homogeneous obstacles. A more worrying case concerns the situation where the unbounded subdomain has a bounded complement. This geometry is typical for scattering problems. As shown in [36, 8], the iteration operator behaves then in a quite different way since for this situation a mode relative to the unbounded domain is neither completely propagative nor completely evanescent. A numerical example is given below to compare this approach with the EMDA.

6. Numerical results

6.1. Validation of the algorithm

Some numerical results, validating the above method, are first presented. We start by testing the behavior of the iterative method with respect to the number of subdomains, the wavenumber, etc... More precisely, consider an annular domain with a constant refractive index $n^2 = \varepsilon = 1$ with radii $R_1 = 1$ and $R_0 = R_1 + 2\pi/k$ where $k = \pi$. The mesh size corresponds to 12 points per wavelength and the damping coefficient (EMDA algorithm) is fixed to $\mathcal{X} = 0.5$ (32).The interface problem is solved using a GMRES solver [24]. The iterations are stopped when the initial residual has decreased by a factor of 10^{-6}. Table I shows that the number of iterations is increasing nearly linearly with the number of subdomains at a rate between 2 an 3. Note that the number of subdomains represented in table I includes Ω_0^∞. Figure 5 compares the solution obtained by the DDM with the approach based on a direct BEM-FEM coupling. The regular behavior at cross-points of the solution delivered by the DDM clearly demonstrates the advantage of the proposed way to handle them.

Let us now consider a partition of the initial domain into 7 subdomains including Ω_0^∞. Our aim now is to bring out the effect of the number of points per wavelength on the number of iterations. As indicated in table II, passing from for 12 to 16 points by wavelength requires 5 additional iterations. The number of iterations continues to moderately grow with the number of points by wavelength until it is about 28 or 30. This indicates that, despite

Subdomains	3	5	7	9	11	13	15	17
Iteration number	32	38	41	45	47	51	54	57

Table I. Number of iterations with respect to the subdomains one.

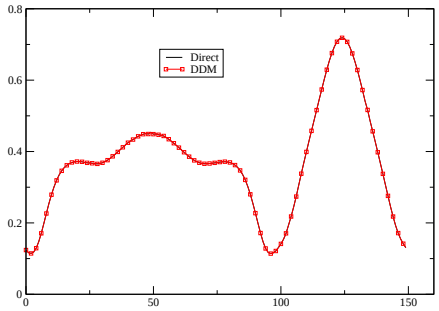

Figure 5. Comparison of the DDM solution with the direct one.

the conclusions that are drawn in some theoretical studies [4, 20], the number of iterations is bounded independently of the mesh in practical computations. A possible explanation of this apparent contradiction can be provided by the fact that practical meshes are unable to represent highly oscillating evanescent modes.

pts/wavelenght	12	16	20	24	28	30
Iteration number	41	46	49	53	56	57

Table II. Number of iterations with respect to the mesh size.

In table III, we now address the dependance of the number of iterations on the frequency, or equivalently here on the wavenumber. For the present experiment, we have kept the previous case and used 12 points per wavelength. Note that the frequency is directly related in this problem to the geometry which can be fixed through the following relation $k(R_0 - R_1) = 3k$. Surprisingly enough, a conclusion, similarly to the number of points by wavelength, the number of iterations seems to be practically bounded relatively to the frequency.

wavenumber	3.14	4	6	8	10	12
Iteration number	32	44	46	48	51	51

Table III. Number of iterations with respect to the wavenumber.

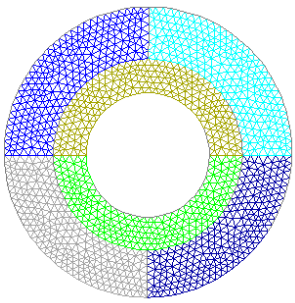

Figure 6. Decomposition of the initial domain into 6 subdomains.

6.2. Absorbing boundary condition

In this subsection, we compare the application of the DDM to the BEM-FEM coupling (16)-(17) with its use as a solving procedure for a plain FEM modelling with an absorbing condition set on a terminating artificial boundary. Two radiations conditions are considered: the crudest radiation condition, directly derived from the classical Sommerfeld radiation condition, and the second order Bayliss-Turkel absorbing boundary condition [33]

$$\partial_{\mathbf{n}} u - iku = 0, \tag{34}$$

$$\partial_{\mathbf{n}} u - iku + \frac{1}{2R}u - \frac{1}{8R^2(1/R - ik)}u - \frac{1}{2(1/R - ik)}\partial_s^2 u = 0. \tag{35}$$

There, R stands for the radius of the circle used to truncate the unbounded domain and ∂_s is the tangential derivative relatively to the arc-length.

We again deal with the above annular domain characterized by R_1 and $R_0 = R_1 + 2\pi/k$. The bounded subdomain with $R_1 < r < R_0$ in polar coordinates is divided in 2 non-overlapping subdomains. In the case of the pure FEM solution, the part of the unbounded domain $R_0 < r < R$ is split into 4 subdomains and finally obtain a decomposition in 6 subdomains (figure 6). Table IV gives for each case of computation the number of iterations which have been necessary for the iterative process to converge and the relative error

$$\text{error} = \frac{\|u - u_{\text{ex}}\|_2}{\|u_{\text{ex}}\|_2},$$

computed relatively to the L^2 norm, using the analytical expression u_{ex} for the solution to the scattering problem available by means of a Fourier-Hankel series (see, for example, [21] where this calculation is reproduced or [26] where a similar one can be found). As expected, the domain decomposition method BEM-FEM is the more accurate. It is also the method which required the lowest number of iterations.

6.3. Residual

It is mentioned in [35] that it is important to find a realistic stopping criterion in order to not carry out iterations which improves the solution of the discrete problem without any true

pts/wavelenght	12		16		20	
$k = \pi$	error in %	Iterations	error in %	Iterations	error in %	Iterations
FEM 1st order RC	6.1	32	4.4	36	4.4	40
FEM 2nd order RC	6.0	33	3.5	37	2.2	41
BEM-FEM	2.9	25	1.4	27	1.0	29

Table IV. Iteration number and relative error.

pts/wavelenght	12		15	
Residual	error in %	Iterations	error in %	Iterations
0.5	142	2	143	2
10^{-1}	24	5	26	5
10^{-2}	6.31	10	4.68	11
10^{-3}	6.23	17	4.58	18
10^{-4}	6.22	25	4.55	26
10^{-5}	6.22	32	4.54	35
10^{-6}	6.22	40	4.54	44

Table V. Iteration number and RCS relative error.

impact on the accuracy of the numerical simulation. Here, we compute the relative error of the radiate wave in the far-field zone with respect to various values for the residual. The behavior of the scattered field for an incident plane wave $u^{\rm inc}$ is generally described by the Radar Cross Section (RCS [39]). More precisely, in the two dimensional case, the bistatic RCS is given by

$$\mathrm{RCS}(\theta) = 10\log_{10}(2\pi|a_0(\theta)|^2),$$

where (r,θ) stands for the polar coordinates. The scattered amplitude $a_0(\theta)$ in the direction θ can be computed from the following formula

$$a_0(\theta) = \frac{\exp\ (-i\pi/4)}{\sqrt{8\pi k}} \int_\Gamma \{\partial_{\mathbf{n}_y} u(y) - ik\mathbf{\Theta}\cdot\mathbf{n}_y\ u(y)\} \exp\left(-ik\ \mathbf{\Theta}\cdot\mathbf{r}_y\right) d\Gamma_y, \tag{36}$$

with $\mathbf{\Theta} = {}^t(\cos\theta, \sin\theta)$ and $\mathbf{r}_y$ is the radius vector of the point y. The analytical value for the RCS is given by means of a Bessel-Hankel Fourier series expansion as above. For this numerical experiment, we have considered the same annular domain as above with a splitting of the FEM 5 subdomains. Table V clearly shows that a residual of order 10^{-3} is enough to reach the maximum accuracy that can be delivered by the approximation process.

6.4. Convergence of the domain decomposition method

This subsection is devoted to the comparison between the EMDA with the algorithm based on the optimization techniques. We choose the OO2 transmission conditions given in [17] for $k = 50$ by

$$S = -ik + (5 + i\ 13)10^{-3}\partial_s^2.$$

To perform this test, we consider the above annular geometry with $k(R_0 - R_1) = 50$. The domain treated by the FEM is decomposed into 8 subdomains and the computation has been

	EMDA	OO2
homogeneous	68	69
non-homogeneous	72	108

Table VI. Iteration number for EMDA and OO2 transmission conditions.

Subdomain	1	2	3	4	5	6	7	8
ε	0.4	0.8	1	1.2	1.4	1.6	1.8	2.0

Table VII. Relative permittivity.

done at 14 points per wavelength. Two simulations have been performed respectively for the homogeneous and for the non-homogeneous case. Table VI shows that in the homogeneous case, the EMDA and the optimization method require almost the same number of iterations. For the non-homogeneous case, the EMDA is faster that the OO2 algorithm. However, at this level, no conclusion can be drawn because the convergence depends on several parameters: geometry, number of subdomains, frequency, etc and it seems to be hard to take all of them into account.

6.5. Other geometries

The previous numerical experiments have been carried out using a particular geometry for which an analytic expression for the solution was available to validate the approach and to get an idea on the reduction of the residual which is needed to obtain an effective error at an acceptable level. We now consider the geometry depicted in figure (7). The domain in which is posed the scattering problem is divided into 25 subdomains (24 bounded subdomains dealt with using the FEM and the unbounded one Ω_0^∞). The wavenumber is fixed to $k = 2\pi$ so that the size of the scatterer is about $8\lambda \times 8\lambda$ where λ is the wavelength. Finally, the mesh size corresponds to 14 points per wavelength and ε and n are fixed to 1. A reduction of 10^{-6} of the initial residual is reached in 75 iterations.

In the case of the geometry represented in figure 8, the domain is divided into 38 subdomains (37 relative to the FEM and the unbounded one). We have taken 14 points per wavelength and $k = 4$. The size is then of $10\lambda \times 13\lambda$. For again $\varepsilon = n^2 = 1$, 82 iterations are required to reduce the residual by a 10^{-6} factor. In the non-homogenous case (see table VIII), the same reduction requires 162 iterations, that is, nearly the double than for the homogeneous case. A plausible explanation is that the used operator $\mathcal{S}$ is designed for homogeneous materials and thus is not probably the most adapted in the non-homogenous case. However, the application of the DDM to solve the BEM-FEM coupling remains more efficient than the direct approach.

The last 2D example presents the following multiple scattering problem

$$\begin{cases} \Delta u + k^2 u = 0, \quad \text{in } \Omega, \\ \partial_{\mathbf{n}} u = g, \quad \text{on } \partial\Omega, \\ \lim\limits_{|x|\to+\infty} |x|^{1/2} \left(\partial_{|x|} u - iku\right) = 0, \end{cases} \tag{37}$$

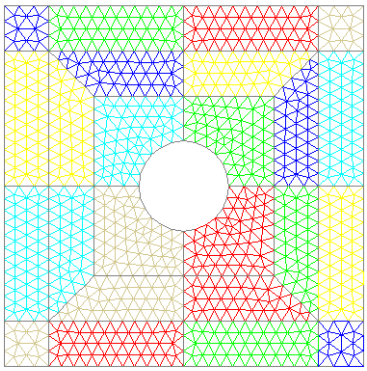

Figure 7. Partition into 25 subdomains.

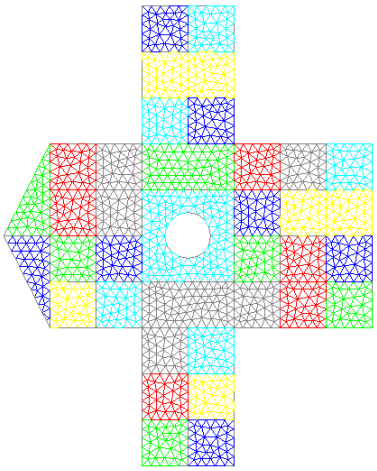

Figure 8. Partition into 38 subdomains.

Subdomain	2,4	5,7	8,10	11,13	14,16	17,19
ε	0.5	0.8	1.1	1.4	1.7	2.0
Subdomain	20,22	23,25	26,28	29,31	32,34	35,38
ε	2.3	2.6	2.9	3.2	3.5	3.8

Table VIII. Relative permittivity.

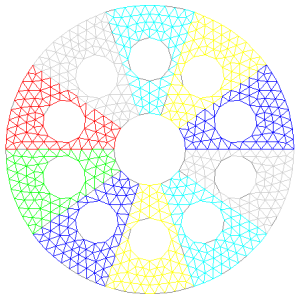

Figure 9. multiple scattering problem configuration:

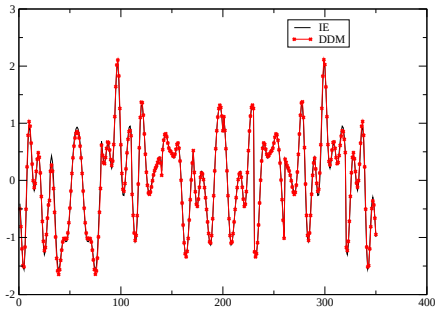

Figure 10. Solution by integral equation and domain decomposition method.

where Ω is an unbounded domain such that its boundary $\partial\Omega$ is the union of the circles Γ_i $(i = 1, \ldots, M = 10)$ depicted in figure 9. The data $g := -\partial_{\mathbf{n}} u^{\text{inc}}$ corresponds to an incident plane wave u^{inc}. Again, $\mathbf{n}$ denotes the outward unit normal to the boundary $\partial\Omega$. The solution can be represented as

$$u(x) = \sum_{i=1}^{M} N_i \lambda_i(x), \quad x \in \Omega,$$

where N_i is the double layer potentiel (8) created by a density λ_i on Γ_i. However, a pure integral equation solution is expensive since all the Γ_i are coupled. The DDM solution of the BEM-FEM formulation has required 66 iterations to obtain a reduction of the initial residual by a factor 10^{-6}. The procedure makes it possible to efficiently solve the scattering problem since it can take advantage much more easily than a pure BEM of its geometrical symmetries without a significant loss of the accuracy (see figure 10 where are depicted the solutions obtained by a direct BEM and the DDM procedure). We have taken $k = \pi$ and 14 points per wavelength for this numerical experiment.

6.6. Some 3D numerical examples

Consider a scattering problem with a geometry similar to the above one in 2D. The scatterer is a hard-sound sphere of radius R_0 equal to $3/4$ of the wavelength λ covered by a shell of penetrable material of relative index $n = 2$ filling the domain $R_0 < |x| < R_1 := \lambda$. For this case too, an analytical expression of the scattered wave is available in terms of a Fourier-Hankel series expansion when the incident field is a plane wave.

We have applied the DDM to solve the coupled FEM-BEM formulation using a decomposition of the shell in successively 80, 100, 144 and 200 domains (see figure 11). For the interface operator, we have simply chosen the EMDA approach with $\mathcal{S} := -ik(1 + i0.5)$. The parameters, characterizing each decomposition, are reported in table IX. The results are reported in the figures 13 and 14. It is important to note that the convergence to the exact solution seems to be almost independent of the mesh in this case and that only 10 to 15 iterations are enough to reach the accuracy that can be delivered by the numerical process for the determination of the far field pattern.

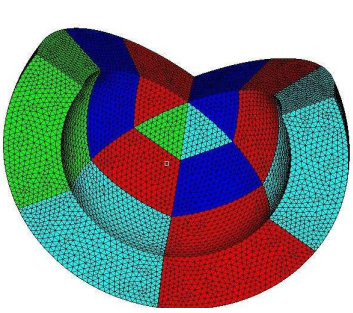

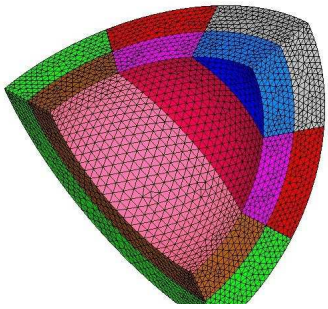

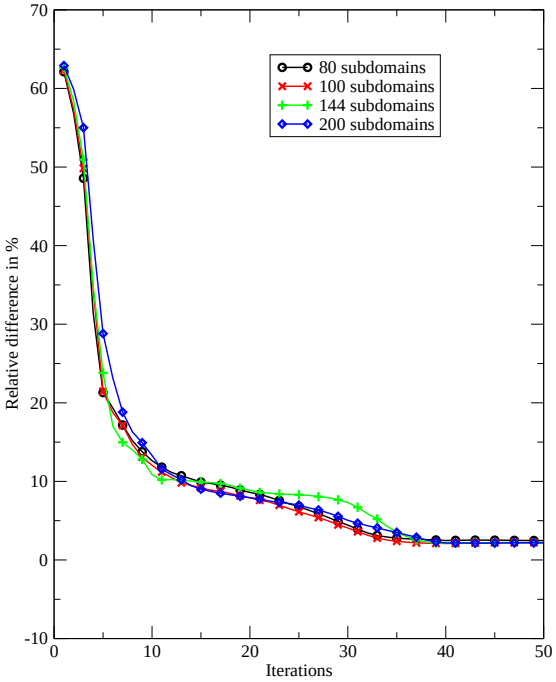

Figure 13. Current relative error.

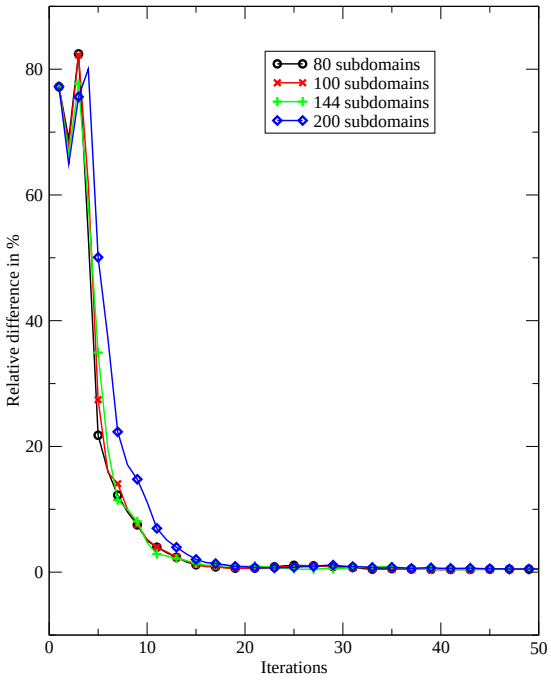

Figure 14. RCS (radar cross section) relative error.

Subdomains	Nodes	Tetrahedrons	Cross-points	Interfaces	IE Matrix
80	262976	1446800	5352	312	25826
100	287034	1581320	6084	390	27582
144	289536	1597248	7500	564	26618
200	312944	1728880	9384	780	29442

Table IX. This table describe, after each decomposition of the initial computational domain, the parameters corresponding to the resulting meshes and then to the size of the local problems.

7. Conclusion

A significant advantage of the domain decomposition methods lies in the resolution of the BE and FE equations separately. The dense linear system resulting form the BE procedure is efficiently solved by the public domain library `SCALAPACK`. For the sparse linear system corresponding to the FE part, the domain decomposition method appears as the best strategy since the utilization for instance of the library `MUMPS`, which is based on a multifrontal method, can exceed the available capabilities in memory storage. The treatment of cross points guarantees the stability and the convergence of the iterative method towards the discrete coupled problem. Various numerical results have shown that the method has performances as good in 2D as in 3D.

REFERENCES

1. V. Rokhlin. *Rapid solution of integral equations of scattering theory in two dimensions,* 1990; J. Comput. Phys, 6(2):414-439.
2. E. Darve. *Méthodes Multipôles Rapides: Résolution Des Équations de Maxwell Par Formulations Intégrales,* 1999; PhD Thesis, Université Paris VI.
3. J. Douglas, F. Fereira and J. E. Santos. *A Parallelizable Approach to the Simulation of Waves in Dispersive Media.* Mathematical and Numerical Aspects of Wave Propagation. Proceedings of the Third International Conference, Mandelieu-La Napoule, France, April 1995, 673–682, SIAM, Philadelphia.
4. F. Collino, S. Ghanemi and P. Joly. *Domain Decomposition Method for Harmonic Wave Propagation: a General Presentation,* 2000; Computer Methods in Applied Mechanics and Engineering, 184:171-211.
5. M.J. Gander, F. Magoulès and F. Nataf. *Optimized Schwarz Methods without Overlap for the Helmholtz Equation,* 2002; SIAM Journal of Scientific Computing, Vol. 24, No 1, pp. 38-60.
6. B. Després. *Méthodes de décomposition de domaine pour les problèmes de propagation d'ondes en régime harmonique. Le théorème de Borg pour l'équation de Hill vectorielle,* 1991; Phd Thesis, Paris VI University, France.
7. B. Stupfel. *A Hybrid Finite Element and Integral Equation Domain Decomposition Method for the Solution of the 3-D Scattering Problem.* J. Comput. Phys., 172(2), 451–471, 2001.
8. Y. Boubendir. *Techniques de Décomposition de Domaine et Méthodes d'Equations Intégrales.* PhD Thesis, INSA of Toulouse, 2002.
9. Y. Boubendir and A. Bendali. *Domain Decomposition Methods for Solving Scattering Problems by a Boundary Element Method.* Proceedings of the 13th International Conference on Domain Decomposition Methods in Lyon, France, 2002, 319–326, CIMNE, Barcelona.
10. B. Després. *Domain decomposition method and the Helmholtz problem,* 1991; Mathematical and numerical aspects of wave propagation phenomena, 44–52, Strasbourg, G. Cohen, L. Halpern and P. Joly. SiAM, Philadelphia, PA.
11. B. Després. *Domain decomposition method and the Helmholtz problem (part II),* 1993; Mathematical and numerical aspects of wave propagation phenomena, pages 197–206, SIAM, Philadelphia, PA.
12. B. Després, P. Joly, J. Roberts. *A domain decomposition method for the harmonic Maxwell's equations,* 1992; In R. Beauvens and P. de Groen, editors, IMACS international symposium on iterative methods in linear algebra, pages 475-484. North Holland-Amsterdam.
13. M Costabel. *Symmetric methods for the coupling of finite elements and boundary elements,* 1987; Boundary Elements IV, Vol.1, Comput. Mech. Brebier Southampton, pp. 441-420.
14. C. Johnson, J.-C. Nédélec. *On the Coupling of Boundary Integral and Finite Element Methods,* 1980; Mathematics of Computation, Volume 35, Number 152, pp. 1063-1079.
15. P.-L. Lions. *On the Schwarz alternating method. III: A variant for nonoverlapping subdomains.* Third International Symposium on Domain Decomposition Methods for Partial Differential Equations, held in Houston, Texas, March 20-22,(1989), 1990; T.F. Chan, R. Glowinski, J. Périaux and O. Widlund, SIAM, Philadelphia, PA.
16. S. C. Brenner. *Analysis of Two-Dimensional FETI-DP Preconditioners by the Standard Additive Schwarz Framework,* 2003; Electronic Transactions on Numerical Analysis, Volume 16, 165–185.
17. F. Magoules, P. Iványi and B. H. V. Topping. *Non-Overlapping Schwarz Methods with Optimized*

Transmission Conditions for the Helmholtz Equations, 2004, Comput. Methods in Applied and Mech. Engrg., volume 193, 4797–4818.
18. C. Farhat, M. Lesoinne, P. L. Tallec, K. Pierson and D. Rixen. *FETI-DP: A Dual-Primal Unified FETI Method—Part I: A Fastr Alternative to the Two-Level FETI Method,* 2001, International J. for Numerical Methods in Engineering, volume 50, 1523–1544.
19. A. Klawonn, O. B. Widlund and M. Dryja. *Dual-Primal FETI Methods for Three-Dimensional Elliptic Problems with Heterogeneous Coefficients,* 2002, SIAM J. of Numerical Analysis, volume 40(1), pages 159–179.
20. A. Bendali and Y. Boubendir. *Non-Overlapping Domain Decomposition Method for a Nodal Finite Element Method,* 2006, Numerisch Mathematik, volume 103(4), 515–537.
21. N. Bartoli and A. Bendali. *Robust and High-Order Effective Boundary Conditions for Perfectly Conducting Scatterers Coated by a Thin Dielectric Layer,* 2002, IMA J. Appl. Math., volume 67(5), 479–508.
22. C. H. Wilcox. *Scattering theory for the d'Alembert equation in exterior domains,* 1975; Volume 42, Springer-Verlag, Berlin.
23. L. Vernhet. *Boundary element solution of a scattering problem involving a generalized impedance boundary condition,* 1999; Math. Meth. Appl., Volume 22, Number 7, pp. 587-603.
24. Y. Saad. *Iterative Methods for Sparse Linear Systems*, PWS, Boston, 1996.
25. William McLean. *Strongly Elliptic Systems and Boundary Integral Equations,* 2000, Cambridge University Press. Cambridge, UK, and New York, USA.
26. J. Van Bladel. *Electromagnetic Fields (Revised Printing),* 1985, Hemisphere Publishing Corporation. New York, Washington, Philadelphia, London.
27. F. A. Milinazzo, C. A. Zala and G. H. Brooke. *Rational Square-Root Approximations for Parabolic Equation Algorithms,* 1997, J. Acoust. Soc. Am., volume 101(2), 760–766.
28. Patrick R. Amestoy, Iain S. Duff, Jean-Yves L'Excellent and Jacko Koster. *A Fully Asynchronous Multifrontal Solver Using Distributed Dynamic Scheduling,* 2002, SIAM Journal on Matrix Analysis and Applications, volume 23(1), 15–41.
29. P. R. Amestoy, I. S. Duff and J.-Y. L'Excellent. *Multifrontal Parallel Distributed Symmetric and Unsymmetric Solvers,* 2000, Comput. Methods in Appl. Mech. Eng., volume 184, pages 501–520.
30. X. Antoine, H. Barucq, A. Bendali. *Bayliss-turkel-like radiation condition on surfaces of arbitrary shape,* 1999; Journal of Mathematics Analysis and Applications, 229:184-211.
31. X. Antoine, A. Bendali and M. Darbas. *Analytic Preconditionners for the Boundary Integral Solution of the Scattering of Acoustic Waves by Open Surfaces*, 2005, Journal of Computational Acoustics, volume 13(3), pages 477–498.
32. Nolwenn Balin, Abderrahmane Bendali, M'Barek Fares, Florence Millot and Nicolas Zerbib. *Some Applications of Substructuring and Domain Decomposition Techniques to Radiation and Scattering of Time-Harmonic Electromagnetic Waves,* 2006, Comptes Rendus Physique, volume 7(5), pages 474–485.
33. A. Bayliss, M. Gunzburger, E. Turkel. *Boundary conditions for the numerical solutions for elliptic equations in exterior regions,* 1982; SIAM J. Appl. Math, 42:430-451.
34. A. Bendali. *Boundary Element Solution of Scattering Problems Relative to a Generalized Impedance Boundary Condition,* 2000, Partial Differential Equations: Theory and Numerical Solution. Proceedings of the ICM'98 Satellite Conference, Prague, Czech Republic. Chapman & Hall/CRC Res. Notes Math., pages 10–24. W. Jäger, J. Nečas, O. John, K. Najzar and J. Stará. Chapman & Hall/CRC Res. Notes Math. Chapman & Hall/CRC, Boca Raton, FL.
35. A. Bendali, Y. Boubendir and M'B. Fares. *A FETI-like domain decomposition method for coupling FEM and BEM in large-size problems of acoustic scattering*, 2007; Computer & Structures, 85:526–535.
36. Y. Boubendir. *An Analysis of the BEM-FEM Non-Overlapping Domain Decomposition Method for a Scattering Problem*, J. Comp. and Applied Math., in press.
37. Y. Boubendir, A. Bendali and F. Collino. *Domain decomposition methods and integral equations for solving Helmholtz diffraction problem.* Pages 760–764, July, 2000. Fifth international conference on mathematical and numerical aspects of wave propagation, SIAM, Philadelphia.
38. L. S. Blackford et al. *ScaLAPACK Users' Guide*, 1997, SIAM, Philadelphia.
39. J. J. Bowman, T. B. A. Senior, P. L. E. Uslenghi and J. S. Asvestas. *Electromagnetic and Acoustic Scattering by Simple Shapes*, 1987. Hemisphere Pub. Corp., New York.
40. G. Chen and J. Zhou. *Boundary Element Methods*, 1992. Academic Press Inc., London.
41. D. Colton and R. Kress. *Integral Equation Methods in Scattering Theory*, 1987. John Wiley and Sons, New York.
42. R. Leis. *Initial boundary value problems in mathematical physics*, 1986, J. Wiley and sons.